Journal of the Korean Physical Society, Vol. 51, No. 3, September 2007, pp. 972∼977

Changes of Electrical Conductivity and Temperature Caused by Electrode Erosion for Atmospheric Plasma Systems

Jong-Chul Lee
School of Mechanical & Automotive Engineering, Kangnung University, Wonju 220-711

Jin-Hyo Boo
Department of Chemistry, Sungkyunkwan University, Suwon 440-746

Youn-Jea Kim*
School of Mechanical Engineering, Sungkyunkwan University, Suwon 440-746

(Received 13 November 2006)

Electrode erosion is indispensable for atmospheric plasma systems, as well as for switching devices, due to the high heat flux transferred from arc plasmas to contacts, but experimental and theoretical works have not identified the characteristic phenomena because of the complex physical processes. In this study, we analyzed the electrical conductivity and the temperature of arc plasmas using the field-coupled computational techniques to consider the electrode erosion in a thermal puffer plasma chamber. Based on the results from the arcing history with metallic vapors, the thermal and electromagnetic characteristics near current zero were investigated using the electrical conductivity and the temperature of the arcing zone. Numerical results showed that the existence of electrode vapors made the arc temperature down during the high-current period and a negative effect with high electrical conductivity on the current interruption.

PACS numbers: 52.65.-y, 52.77.Fv, 47.11.-j
Keywords: Atmospheric thermal plasma, CFD, Electrode erosion, Nozzle ablation, Metallic vapor

I. INTRODUCTION

Electrode erosion is indispensable for atmospheric plasma systems, as well as for switching devices, due to the high heat flux transferred from arc plasmas to contacts [1–4], but experimental and theoretical works have not identified the characteristic phenomena because of the complex physical processes. The thermal plasma generated between metal electrodes causes electrode erosion and metallic vapors from the surfaces. The metallic vapors with high electrical conductivities change the thermodynamic and transport properties of working gas and its insulating properties through the diffusion process.

A nozzle arc device [5] is usually used to simplify a gas circuit breaker for simulations, as well as experiments, because the former is the core part of the latter. Zhang *et al.* [6] investigated the effects of electrode vapor on the behavior of a steady-state arc in a supersonic nozzle. Liau *et al.* [7] performed a numerical simulation of a SF_6 arc with copper vapors within a Laval nozzle. Chevrier *et al.* [8] studied the arc-contact interaction in a SF_6 self-blast circuit breaker with the model, which is macroscopic and is based on an energy balance at the boundary between the electrical arc and the electrode.

In this study, we use the field-coupled computational techniques in Section II to analyze the electrical conductivity and the temperature of arc plasmas and to consider the electrode erosion in a thermal puffer plasma chamber. Based on the arcing history with metallic vapors [9], in Section III, the thermal and electromagnetic characteristics near current zero re investigated by using the electrical conductivity and the temperature of the arcing zone. It is concluded in Section IV that the existence of electrode vapors makes the arc temperature down during the high-current period and a negative effect with high electrical conductivity on the current interruption, which plays an important role in the interruption capability of switching devices.

II. NUMERICAL METHODS

Due to the effects of the electromagnetic forces on thermal plasmas, two different types of governing equations should be coupled for analyzing the thermal plasma and

*E-mail: yjkim@skku.edu; Fax: +82-31-290-7448

Table 1. ϕ, Γ_ϕ and S_ϕ for the governing equations.

Equations	ϕ	Γ_ϕ	S_ϕ
Mass	1	0	0
Radial momentum	v	$\mu_l + \mu_t$	$-\frac{\partial p}{\partial r} + (J \times B)_r + (\mu_l + \mu_t)\nabla^2 v - \frac{2(\mu_l+\mu_t)v}{r^2}$
Axial momentum	w	$(\mu_l + \mu_t)$	$-\frac{\partial p}{\partial z} + (J \times B)_z + (\mu_l + \mu_t)\nabla^2 w$
Enthalpy	h	$(k_l + k_t)/c_p$	$\frac{dp}{dt} + \sigma E^2 - q + (\mu_l + \mu_t)\left(\frac{\partial v_i}{\partial x_j} + \frac{\partial v_j}{\partial x_i}\right)\frac{\partial v_i}{\partial x_j}$
PTFE concentration	c_{PTFE}	$\rho(D_l + D_t)$	0
Metal vapor concentration	c_{Cu}	$\rho(D_l + D_t)$	0

the flow characteristics. One is Navier-stokes equations for the thermal-flow field, and the other is Maxwell's equations for the electromagnetic field.

Eq. (1) shows the conservation equations written in cylindrical polar coordinates for the thermal-flow field, and the electric potential is found from Eq. (2) for the conservation of current:

$$\frac{\partial}{\partial t}(\rho\phi) + \frac{1}{r}\frac{\partial}{\partial r}\left[r\rho\vec{V}\phi - r\Gamma_\phi\frac{\partial\phi}{\partial r}\right] + \frac{\partial}{\partial z}\left[\rho\omega\phi - \Gamma_\phi\frac{\partial\phi}{\partial z}\right] = S_\phi, \quad (1)$$

$$\frac{1}{r}\frac{\partial}{\partial r}\left(r\sigma\frac{\partial\varphi}{\partial r}\right) + \frac{\partial}{\partial z}\left(\sigma\frac{\partial\varphi}{\partial z}\right) = 0, \quad (2)$$

where ϕ is the scalar variable, Γ_ϕ the diffusion coefficient, S_ϕ the source terms, φ the electric potential and σ the electrical conductivity. Further information for the governing equations is listed in Table 1.

The azimuthal magnetic field is generated by the current flowing through the arc plasmas between the electrodes. The field is expressed by Ampere's circuital law:

$$\frac{1}{r}\frac{\partial}{\partial r}(rB_\theta) = \mu_0 j_z, \quad (3)$$

where μ_0 is the permeability of the arc plasma ($=4\pi \times 10^{-7}$ H/m). The field generates Lorentz forces, which are related with the behavior of the arc plasma itself and the flow characteristics, with current densities.

Due to the high arcing current and strong radiation, an ablation of PTFE nozzles and an evaporation of metal electrodes occur. For the radiation modeling of arc plasmas, the net emission coefficient (NEC) based on pure SF_6 [10] is used for the approximate radiation model [11] because the radiation emission from the mixture is not known. The modeling result for the ablation of PTFE nozzles is given in Ref. 10. The rate of ablation of PTFE nozzle is determined by

$$\dot{m}_{PTFE} = \frac{F(1-\alpha)Q}{h_a}, \quad (4)$$

where Q is the total radiation flux, α the reabsorption factor, h_a the depolymerization energy ($=1.19 \times 10^7$ J/kg), and F the empirical factor ($=0.9$). This means that the amount of ablated PTFE is proportional to the amount of radiation reaching the nozzle. It is assumed that the velocity at which the vapor is injected depends on the mass flow rate and the density and that the temperature of the vapor is around 3,400 K.

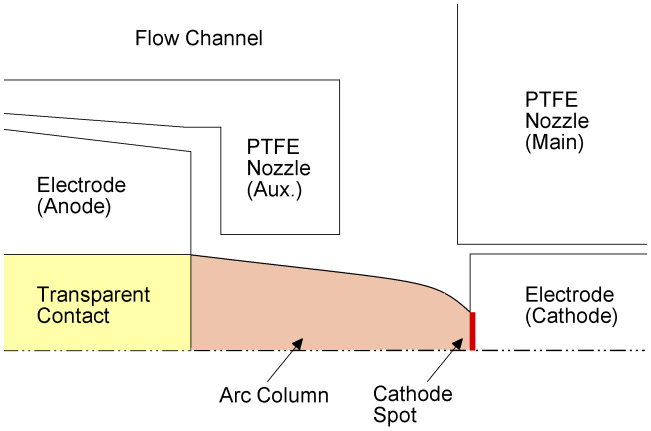

Fig. 1. Arrangement of the arc column and the cathode spot between the electrodes. Evaporation can be produced only on the cathode surface because the anode is a hollow contact with a transparent contact in this apparatus.

In order to consider the effect of electrode evaporation, we firstly approximate the cathode spot [13], where the arcing current is collected in a circular area and the metallic vapor is evaporated, as shown in Figure 1. We assume that the evaporation happens only at the cathode due to the complex physical phenomena of arc rooting inside a hollow anode. The rate of evaporation of the Cu electrode happens to reach the melting temperature (≈1,356 K for copper) of the cathode surface and to produce the following:

$$\dot{m}_{\mathrm{Cu}} = q_v / h_v, \quad (5)$$

where h_v is the total energy required to heat up the electrode surface to the melting temperature (=135 kJ/kg) and to supply the latent heat for phase change per a unit mass (=5,070 kJ/kg) of the cathode material. q_v is the energy available for vaporization of the Cu electrode. We assume that the velocity at which the vapor is injected depends on the mass flow rate and the density and that the temperature of the vapor is around 1,356 K.

The pressure of the arc plasma is above atmospheric

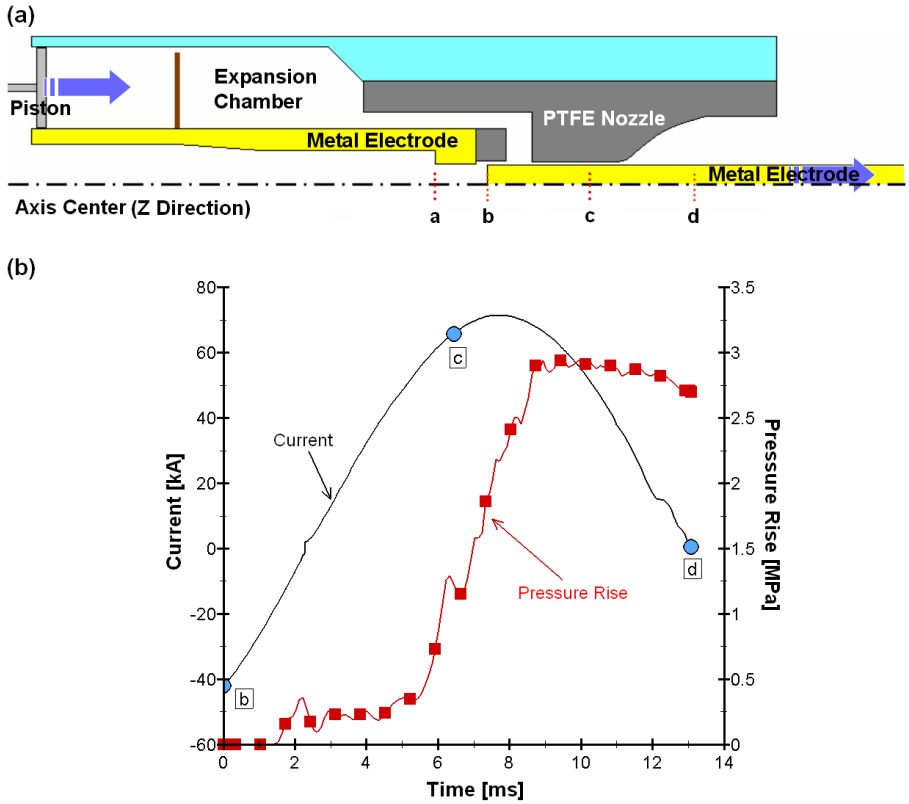

Fig. 2. (a) Schematic diagram of a thermal puffer interrupter and (b) the applied current waveform and the pressure rise used for the simulations. The key locations are indicated by letters "a" to "d". The radius of the metal electrode is 10 mm.

pressure; thus, particle collisions (atomic, molecular, ions and electrons) are frequent and the plasma is said to be collision dominated. Under these conditions, the arc plasma is in local thermodynamic equilibrium (LTE), and all particles have a single temperature. Local chemical equilibrium (LCE) can be used to simplify the calculation of the composition of the mixture and the diffusion coefficients of the vapors [14]. The composition of the mixture is obtained by minimization of the Gibb's free energy under the assumptions of LTE and LCE. The thermodynamic and transport properties are then calculated by using basic transport theory and are tabulated as functions of the temperature, the total pressure of the mixture, and the mass concentration of PTFE vapor. The electrical conductivity of the mixture is used from the data of Chervy *et al.* [15] due to the much higher electrical conductivity of copper vapor.

For turbulent modeling of arc plasmas, the modified Prandtl's mixing length model, which was developed and verified on nozzle arc devices by Yan *et al.* [16], is used. The length scale is proportional to the local thermal radius, which characterizes the boundary of the high-velocity core. The eddy viscosity can be calculated by using

$$\mu_t = \rho(c_1\delta)\left[2\left(\frac{v}{r}\right)^2 + \left(\frac{\partial w}{\partial r} + \frac{\partial v}{\partial z}\right)^2\right], \qquad (6)$$

where δ is the thermal radius and c_1 is a turbulence parameter (=0.2).

III. RESULTS AND DISCUSSION

Since the existence of metallic vapors can change the electrical conductivity and the temperature between the electrodes, the interpretation of the physical interaction caused plays an important role in the design of atmospheric plasma systems, as well as switching devices. The present calculation model is the thermal puffer plasma chamber used widely in high-voltage switching devices, as shown in Figure 2(a). It consists of a pair of metal electrodes (anode and cathode) for current flow, PTFE nozzles for insulation and ablation, and two chambers (compression and expansion). The pressure transients in two chambers are produced by the mechanical piston and by the entrained thermal energy from the arcing zone, respectively. Since the pressure rise in the compression chamber is for the interruption of a small current, we focus on the pressure rise in the expansion chamber for the extinction of a high current. Figure 2(b) shows the pressure rise inside the expansion chamber with the applied current waveform. The key locations are indicated by letters "a" to "d". The pressure in the expan-

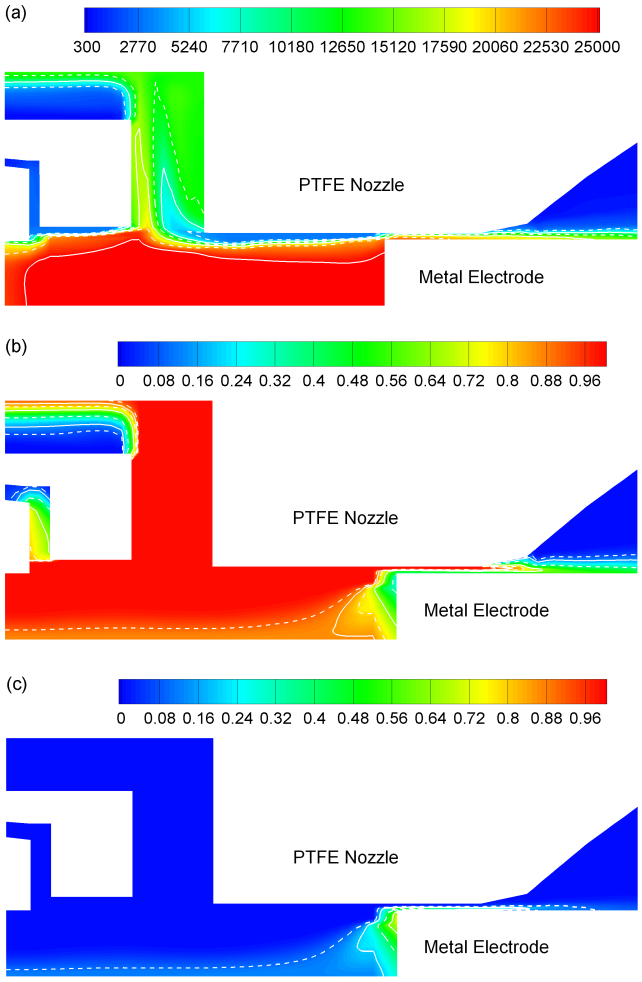

Fig. 3. Distributions of (a) temperature, (b) PTFE vapor concentration and (c) Cu concentration in the arcing zone (AZ) at the key location "c".

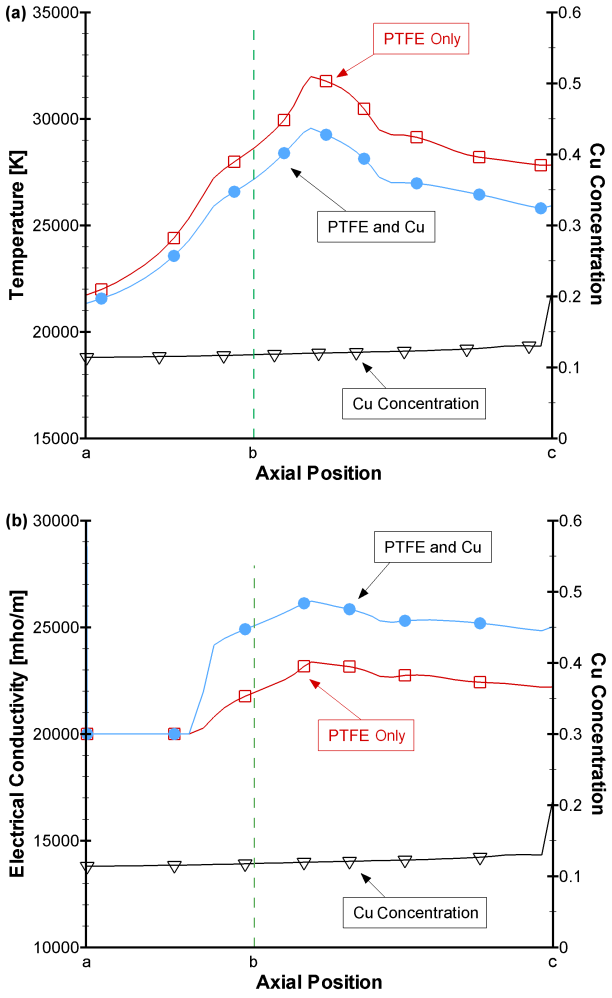

Fig. 4. Temperature, electrical conductivity, and Cu concentration profiles along the z-axis at the key location "c": (a) temperature and (b) electrical conductivity.

sion chamber is shown to increase with the elevation of current to time "c" by the energy inflow from the arc plasma. Due to nozzle blocking, it continues to around 9 ms. After around 9 ms, it starts to flow out reversely from the expansion chamber because of the cooling of the arc plasma between the electrodes.

The thermal energy of the arc plasma is used for heating of the working gas, PTFE nozzles, and electrode. The energies for inducing ablation and evaporation are provided by the power radiated from the arc plasma to the nozzle surface and by the effective thermal flux from the arc plasma to the cathode, respectively, as mentioned above. In order to analyze the thermal characteristics during the high-current period, the distributions of temperature and PTFE and Cu concentrations at time "c" in the arcing zone (AZ) are shown in Figures 3(a)-(c). In Figure 3(b), severe ablation occurs in the vicinity of the nozzle throat where the radiative flux density at the surface is most severe owing to the closer proximity of the surface to arc plasmas. Also the generated PTFE vapors entrain into the expansion chamber through the flow channel by a diffusion process and produce an additional pressure elevation in the chamber. In Figure 3(c), electrode evaporation happens over the full area of the electrode tip because the magnitude of current is full enough at time "c". For the intensity of PTFE vapors, the concentration of the metallic vapors near the axis center is much higher than anywhere. It can be a problem to decrease the dielectric strength between the electrodes due to the high electrical conductivity of the metallic vapors unless the gas flow performs moderately near current zero.

In order to investigate the effect of metallic vapors during the high-current period, we show the axial temperature and the electrical conductivity profiles with Cu concentration between locations "a" and "c" at time "c" are in Figures 4(a)-(b), respectively. The Cu concentration is almost uniform between the locations, except for the region of the cathode tip. Near the cathode tip, the Cu concentration starts to decrease quickly as a result

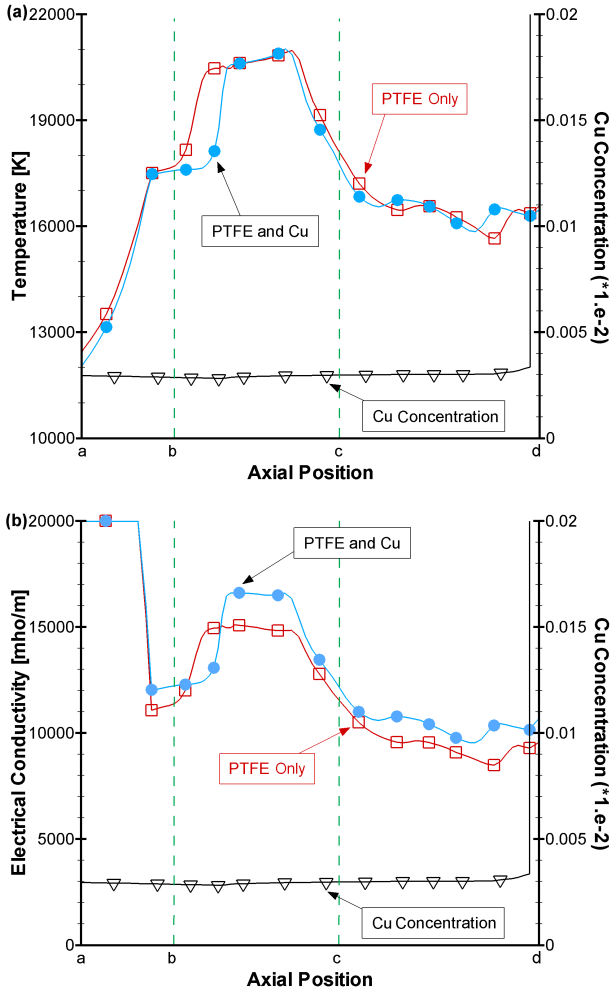

Fig. 5. Temperature, electrical conductivity and Cu concentration profiles along the z-axis at the key location "d": (a) temperature and (b) electrical conductivity.

of the accelerating axial flow and the strong turbulent diffusion, which is the same trend as in Ref. 10. In the majority of the arc column, the Cu concentration is about 13 %. The highest Cu concentration is about 30 % near the cathode tip. The metallic vapor affects the temperature of an arc plasma. In the case of PTFE ablation and Cu evaporation (solid circular symbols), the axial temperature is lower than that of PTFE ablation only (open square symbols), as shown in Figure 4(a). Also, as shown in Figure 4(b), the axial electrical conductivity is higher than that of PTFE ablation only due to the metallic vapors. It is noted that the existence of metallic vapors decreases the electrical resistance of the arc column related with Joule heating, which is used as the energy input of arc plasmas and the pressure rise in the chamber.

When the applied current becomes 100 A at time "d", the axial temperature and the electrical conductivity profiles with Cu concentration between the locations "a" and "d" are shown in Figures 5(a)-(b), respectively.

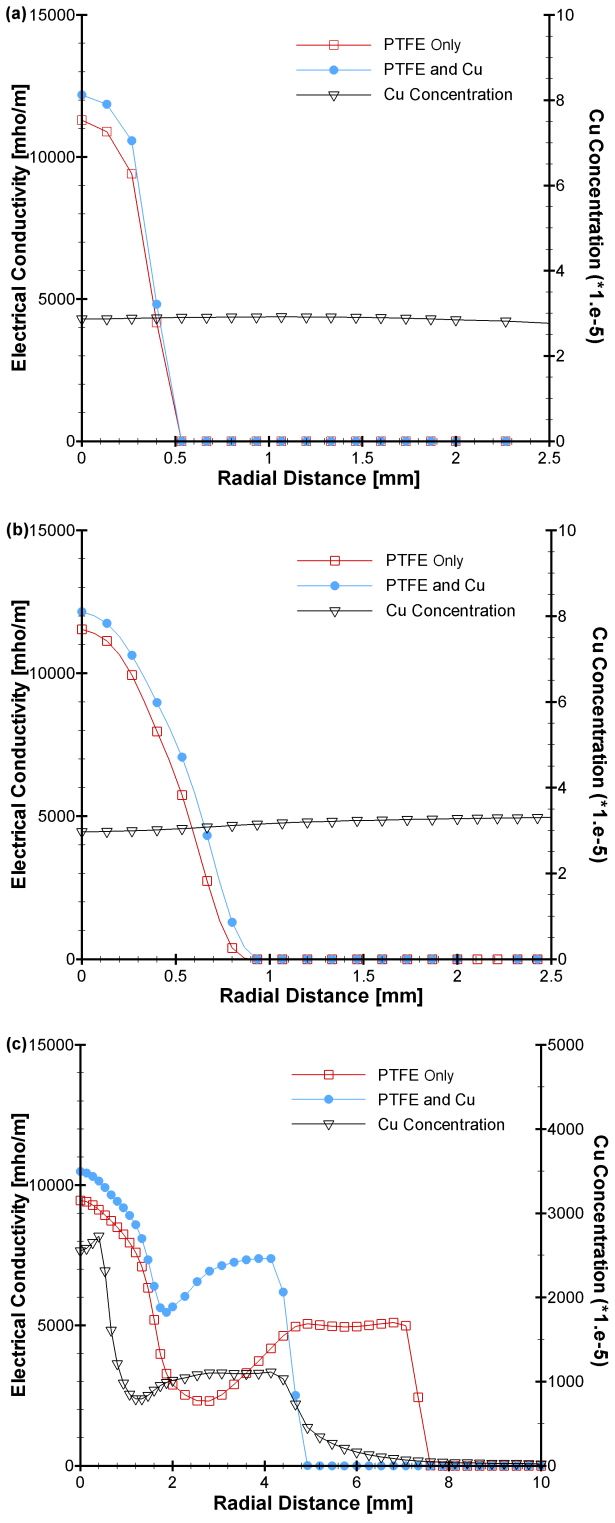

Fig. 6. Electrical conductivity and Cu concentration profiles along the radial direction to (a) the point "b", (b) the point "c", and (c) the point "d" at the key location "d".

In the majority of the arc column, the Cu concentration decreases drastically and is about 0.003 % due to the gas blowing due to the pressure gradient from the

expansion chamber. However, the highest Cu concentration near the cathode tip is about 5 %, which should be very sensitive to the dielectric strength of the system. Unlike the results at time "c", there is no temperature difference between the two cases, which is not due to the non-existence of metallic vapor but to less blowing-off force from the chamber due to the pressure gradient. It has been noticed in a previous study [9] that the pressure rise inside the chamber with PTFE and Cu is less than that for PTFE only. For the electrical conductivity, the case with PTFE and Cu is slightly higher than that for PTFE only due to the existence of metallic vapor, although the rate of metallic vapor is very small.

In Figures 6(a)-(c), the electrical conductivity and the Cu concentration near current zero (=100 A) are plotted along the radial direction at the three key locations, "b", "c" and "d". From these figures, the arc radii of the arc plasmas are found to be about 0.5 mm, 0.8 mm and 5 mm, respectively. The existence of metallic vapors influences the electrical conductivity of the arc plasma due to the high electrical conductivity as shown in Figure 6(c). Since the high-conductivity condition between the electrodes near current zero might have a negative effect on successful interruption of switching devices, a consideration of metallic vapors should play an important role in research and developments of such systems. Further quantitative studies and verification of these phenomena should follow.

IV. CONCLUSION

The electrical conductivity and the temperature of arc plasmas considering the electrode erosion in a thermal puffer plasma chamber are investigated numerically by using field-coupled computational techniques. Computational results show that the existence of electrode vapors makes the arc temperature down during the high-current period. In addition, electrode evaporation happens over the full area of the electrode tip because the magnitude of current is full enough during the high-current period. For the intensity of PTFE vapors, the concentration of the metallic vapors near the axis center is much higher than it is anywhere else. Near current zero, the Cu concentration decreases drastically and is about 0.003 % due to the gas blowing caused by the pressure gradient from the expansion chamber. However, the highest Cu concentration near the cathode tip is about 5 %, which should be very sensitive to the dielectric strength of the system. Since the high-conductivity condition between the electrodes near current zero might have a negative effect on successful interruption of switching devices, consideration of metallic vapors should play an important role in research and developments of such systems. Further quantitative studies and verification of these phenomena should follow.

ACKNOWLEDGMENTS

The author Jong-Chul Lee acknowledges Professor M. T. C. Fang, Drs. J. D. Yan and C. M. Dixon of the University of Liverpool, England, for technical support and thoughtful guidance during the co-work. The authors Jin-Hyo Boo and Youn-Jea Kim acknowledge the partial financial aid from the Center of Excellency Program of the KOSEF/MOST through the Center for Advanced Plasma Surface Technology (CAPST, Grant No. R-11-2000-086-0000-0) at Sungkyunkwan University.

REFERENCES

[1] M. I. Boulos, P. Fauchais and E. Pfender, *Thermal Plasmas, Fundamentals and Applications* (Plenum Press, New York, 1994).
[2] V. A. Riaby, V. Y. Plaksin, J. H. Kim, Y. S. Mok and H. J. Lee, J. Korean Phys. Soc. **48**, 1696 (2006).
[3] J. H. Park, N.-E. Lee, J. C. Lee, J. S. Park and H.-D. Park, J. Korean Phys. Soc. **47**, 422 (2005).
[4] Y. S. Bae, W. C. Lee, K. B. Ko, Y. H. Lee, W. Namkung and M. H. Cho, J. Korean Phys. Soc. **48**, 67 (2006).
[5] K. D. Song, B. Y. Lee and K. Y. Park, J. Korean Phys. Soc. **45**, 1537 (2004).
[6] J. L. Zhang, J. D. Yan and M. T. C. Fang, IEEE Trans. Plasma Sci. **32**, 1352 (2004).
[7] V. K. Liau, B. Y. Lee, K. D. Song and K. Y. Park, J. Phys. D: Appl. Phys. **39**, 2114 (2006).
[8] P. Chevrier, C. Fievet, S. S. Ciobanu, C. Fleurier and P. Scarpa, J. Phys. D: Appl. Phys. **32**, 1494 (1999).
[9] J. C. Lee and Y. J. Kim, Vacuum **81**, 875 (2007).
[10] R. W. Liebermann and J. J. Lowke, J. Quant. Spectrosc. Radiat. Transfer **16**, 253 (1976).
[11] J. F. Zhang, M. T. C. Fang and D. B. Newland, J. Phys. D: Appl. Phys. **20**, 368 (1987).
[12] J. L. Zhang, J. D. Yan, A. B. Murphy, W. Hall and M. T. C. Fang, IEEE Trans. Plasma Sci. **30**, 706 (2002).
[13] K. C. Hsu, K. Etemadi and E. Pfender, J. Appl. Phys. **54**, 1293 (1983).
[14] A. B. Murphy, J. Phys. D: Appl. Phys. **29**, 1922 (1996).
[15] B. Chervy, A. Gleizes and M. Razafinimanana, J. Phys. D: Appl. Phys. **27**, 1193 (1994).
[16] J. D. Yan, K. I. Nuttall and M. T. C. Fang, J. Phys. D: Appl. Phys. **32**, 1401 (1999).